RESEARCH

Detection of Optic Disk Based on Saliency Map

Zhun Fan[1*†], Yibiao Rong[1], Xinye Cai[2], Heping Chen[3], Weihua Sheng[4] and Fang Li[1]

*Correspondence: zfan@stu.edu.cn
[1] Key Laboratory of Digital Signal and Image Processing of Guangdong Province, School of Engineering, Shantou University, Guangdong, China.
Full list of author information is available at the end of the article
†Equal contributor

Abstract

Detecting the optic disk (OD) is very important for the fundus image analysis. In this paper, we propose an algorithm which allows us to automatically segment the optic disk from a fundus image. The method proposed for the extraction of the optic disk contour is mainly based on the saliency map, which can make the OD more prominent in the fundus image. After the saliency map of the fundus image is obtained, threshold processing is performed on the saliency map to obtain the region which includes the optic disk center. Then we search the fittest center in the region and approximate the optic disk contour by a circle. The implemented algorithm has been validated on the public dataset Digital Retinal Images for Optic Nerve Segmentation (DRIONS). The average values obtained (an accuracy of 100%, area over lap of 0.7933, true positive and false positive fraction of 0.8909 and 0.1350, mean absolute distance of 6.1031) demonstrate that the method is feasible and effective for automatic segmentation of the optic disk.

Keywords: Detection of optic disk; Saliency map; Fundus image

Introduction

It is very important to detect the OD accurately not only in analyzing fundus image but also in computer aided diagnosis of different types of eye diseases such as glaucoma. In particular, detecting OD is often a key step for detecting anatomical structures[1] [2]. For example, locating the OD helps avoid false positive in the detection of exudates associated with diabetic retinopathy, since both of them are regions with similar intensity [3]. Besides, the vessels, which are of direct importance in assessing vascular condition, radiate from the OD, which may in many cases serve as a starting point for vessel tracking algorithms [2]. In addition, the OD is crucial in localization of the fovea, the central part of the retina that subserves fine vision [2].

Generally, the presented methods for OD segmentation can be categorized into three groups: template-based methods, deformable models, and morphological algorithms [3]. In the group of the template-based methods, Park et al [4] and Aquino et al [5] used the edge detection followed by the Circular Hough Transform to detect the OD. Lalonate et al [6] proposed a method for the OD segmentation using pyramidal decomposition and Hausdorff-based template matching. Color decorrelated is used to detect the OD in [7]. Concerning the deformable models, Osareh et al [8] used an Active Contour Model based on the Gradient Vector Flow (GVF), so called GVF snake to detect the OD boundary. Li et al [9] introduced an active shape model for the OD segmentation. Lowell et al [2] modified the active contours by exploiting specific features of the OD anatomy. In the third group, most of the morphological algorithms detect the OD by means of watershed transformation.

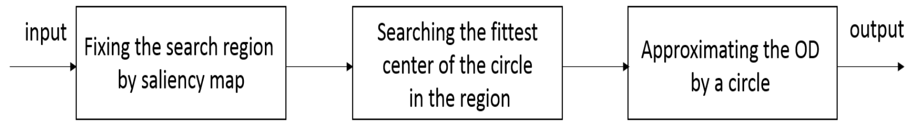

Figure 1 The flow chart of the proposed algorithm. In the first step, the search region is fixed by saliency map, then searching the fittest center of the circle on the fixed region. Finally, the OD boundary is approximated by a circle.

Walter et al [10] detected OD by maker-controlled watershed. Moeales et al [3] used the stochastic watershed to detect the OD. Welfer et al [11] proposed an adaptive morphological approach to segment the OD.

Most of the above methods utilize the edge information of the OD to detect it. However, when the edge blurs or uneven illumination occurs in the image, these methods may fail to locate the OD correctly. In addition, most of them need to eliminate the vessels due to the fact that the vessels have strong negative impact to these methods when detection of OD is performed. In this paper, we proposed a new algorithm for detecting the OD based on the saliency map. Because the proposed method utilizes the region information as the main source to detect the OD, it is not sensitive to the edge variations. In this method, the vessels are also integrated as region information to enhance the method, so there is no need for the algorithm to take extra steps to eliminate them. The experimental results demonstrate that the proposed method is feasible and effective to detect the OD. The flowchart of the proposed method is shown in Fig.1.

The remainder of the paper is organized as follows. In Section II the proposed method is presented. The experimental results are given in Section III and discussed in Section IV. Some concluding remarks are drawn in Section V finally.

METHOD

Saliency Map

The purpose of the saliency map is to represent the conspicuity - or saliency- at every location in the visual field by a scalar quantity and to guide the selection of attended locations, based on the spatial distribution of saliency [12]. Obtaining the saliency map of an image can be conducted in three steps [13]. First, feature vectors are extracted at locations all over the image plane. Second, an activation map is formed by using the feature vectors. Third, the activation map is normalized to highlight conspicuity and admit combination with other maps. Harel et al proposed a Graph-Based Visual Saliency (GBVS) in [13], which is more reliable compared with the standard methods, such as the one proposed by Itti [12].

The algorithm of GBVS is described as follows. First, forming the feature map M by convolution of the image with the linear filters followed by half-wave rectification [13] [14]. Then to highlight the locations (i, j) which are somehow unusual to their neighborhood in the feature map M, the dissimilarity between (i, j) and (p, q) is defined as follows:

$$d((i,j)|(p,q)) = \log(|\frac{M(i,j)}{M(p.q)}|) \quad (1)$$

By connecting every node of the lattice M, a directed graph G_A is formed. A weight to the directed edge from node (i, j) to node (p, q) is assigned as follows:

$$W_1((i, j), (p, q)) = d((i, j)|(p, q))F(i - p, j - q) \tag{2}$$

where $F(a, b) = \exp(-\frac{a^2+b^2}{2\sigma^2})$,and σ is a free parameter. Based on the graph G_A, a Markov chain can be defined by normalizing the weight, which gives us the opportunity to compute the equilibrium distribution over the nodes. The equilibrium distribution accumulates mass at nodes that have high dissimilarity with their surrounding nodes and forms the activation map A [13]. Finally, to concentrate the mass on the activation map A, a graph G_N is formed by connecting every node of the lattice A, and assigning a weight for the edge from node (i, j) to node (p, q) as follows:

$$W_2((i, j), (p, q)) = A(i, j)F(i - p, j - q) \tag{3}$$

Treating the graph as a Markov chain and computing the equilibrium distribution over the nodes, the mass will flow to those nodes which have high activations [13].

Since the OD is generally more prominent in the fundus image, we converted the fundus image into a saliency map using the method proposed by Harel et al [13]. Fig.2 gives a typical example of the experimental results, from which it can be observed that after the saliency map for the fundus image is obtained, as shown in Fig.2.(b), the OD location is more notable. If threshold processing is further performed on the saliency map to get a binary image as shown in Fig.2.(c), it can be seen clearly that most of the pixels in the bright area are located in the OD region, as is demonstrated in Fig.2.(d). From this typical example, it can be concluded that the idea of using saliency map can be very helpful in detecting the OD, and is thus adopted as a main step in the work of this paper.

Detecting the OD

If we assume that the OD can be approximated by a circle with the radius R known, then we can realize the detection of OD by just searching the center of the circle (x_c, y_c). As most of the pixels in the bright region of the binary image of the saliency map are located in the OD, they must include a point which is most suitable to be selected as the center of the circle.

Given a fundus image an intensity image I is usually first derived. As the green component I_g of the fundus image contains most structural information of the OD, we use the I_g as the intensity image for further processing. Since the OD appears as the brighter region in the I_g, the pixels in the OD should have larger intensity values. This also means that the region of the circle should contain most of the brightest pixels, i.e. their intensity values greater than a threshold T_1 , when the OD is approximated best by the circle. Based on this assumption, the search processing of the center (x_c, y_c) can be reformulated as an optimization problem as follows:

$$(x_c, y_c) = \max_{(x_i,y_i)\in\Omega} \{N[(x_i, y_i)|T_1, I_g]\} \tag{4}$$

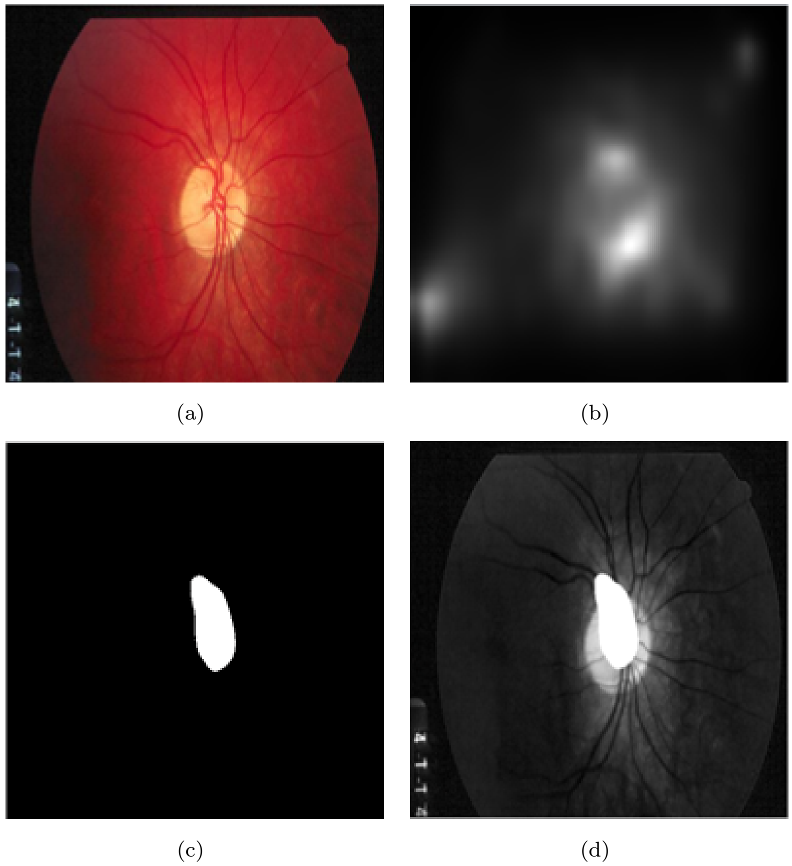

Figure 2 A typical illustration of using the saliency map to process the fundus image: (a) The original fundus image; (b) The saliency map of the original fundus image; (c) The binary map after the threshold processing of the saliency map; (d) Superimposing the binary map on the green channel of the original fundus image.

where Ω is the bright region of the binary image obtained from the saliency map as illustrated by Fig.2, (x_i, y_i) represents an arbitrary point in the Ω , and $N[(x_i, y_i)|T_1, I_g]$ denotes the number of pixels with the intensity values greater than a threshold T_1 in the circle with (x_i, y_i) as the center in I_g. However, since uneven illumination can be presented in some fundus images, if we only use the pixels intensity information, the circle may be biased towards the false region caused by the uneven illumination occuring in the fundus image. To overcome this drawback, Sobel operator [15] is used to integrate the vessels as the region information based on the fact that the vessels radiate from the OD no matter the illumination is even or not.

It is assumed that H_h, H_v, H_{+45}, H_{-45} denote the Sobel operators with size 3×3 in the horizontal, vertical, positive $45°$ angle and negative $45°$ angle direction respectively. If we perform the processing of the I_g using the following Equation (5), we can obtain an enhanced image I_{vessel} in which the vessels are effectively highlighted:

$$I_{vessel} = [\sum_i (H_i \bigoplus I_g)]^{1/2} \tag{5}$$

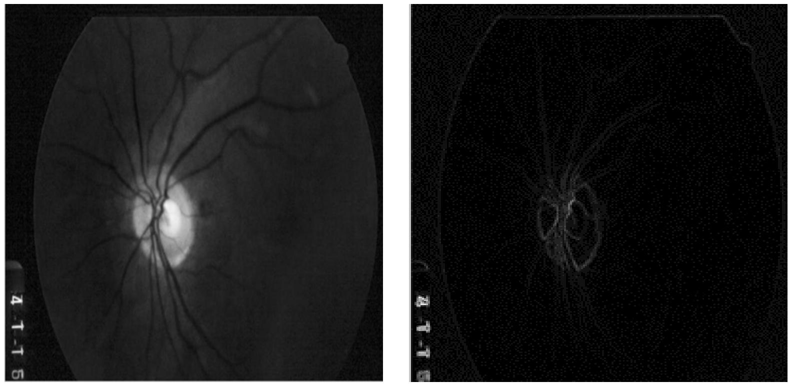

(a) (b)

Figure 3 Enhancing the original image using Sobel operators: (a) The original image I_g ; (b) The enhanced image I_{vessel}.

Where $\bigoplus$ denotes convolution operator, i represents different Sobel operators. Fig.3 gives an example of the experimental result with Fig.3.(a) presenting the I_g , and Fig.3.(b) showing the enhanced image I_{vessel}. It is notable that the vessels are effectively highlighted and their pixels generally have larger intensity value in the I_{vessel}.

Even though the boundary of the OD is also highlighted, we can still use it to search for the center of the circle that can best approximate the OD, since the boundary is also a vital part of the OD. Because we have fixed the search range of the center of the circle by the saliency map, and previously used the original image to locate the center of the circle, we can apply a similar approach to locate the center of the circle by using I_{vessel} with the condition that a separate threshold T_2 needs to be defined accordingly. In summary, by combining Equation (4) and Equation (5), the search of center can be formulated as Equation (6):

$$(x_c, y_c) = \max_{x_i, y_i \in \Omega} \{N[(x_i, y_i)|T_1, I_g] + N[(x_i, y_i)|T_2, I_{vessel}]\} \tag{6}$$

Where $N[(x_i, y_i)|T_2, I_{vessel}]$ denotes the number of pixels with the intensity value greater than the threshold T_2 within the circle with (x_i, y_i) as the center in the image .

Table 1 Visual characteristic of DRIONS database.

Characteristics	Number of Images
Light Artifact	3
Rim Blurred or Missing	5
Moderate Peripapillary Atrophy	16
Concentric Peripapillary Atrophy	20
Strong Pallor Distractor	6

RESULTS

The validation of the method has been carried out on the public dataset DRIONS [16]. In this dataset, there are totally 110 fundus images of 600×400 pixels with their OD manually segmented by two different specialists. The mean age of the patients is 53.0 years old, with 46.2% male and 53.8% female and all of them are Caucasian ethnicity. 23.1% patients had chronic simple glaucoma and 76.9% eye hypertension. Some of the 110 images contain visual characteristics related to potential problems that may distort the detection process of OD-contour. Table 1 [16] shows the number of the images with different potential problems.

The performance of the method is evaluated using different metrics. First, the detection of the OD is defined as correct if the detected OD center lies within the OD boundary [1], which can be used to measure the accuracy of detecting the OD. Second, area overlap (AOL) is defined by Equation (7), which can be further illustrated by Figure (4), where FN denotes false negative, TP denotes true positive, and FP false positive. The AOL is defined as follows:

$$AOL = TP/(TP + FP + FN) \tag{7}$$

According to the Fig.(4), the true positive fraction (TPF) and false positive fraction (FPF) can also be defined [3]:

$$TPF = TP/(TP + FN) \tag{8}$$

$$FPF = FP/(TP + FN) \tag{9}$$

Another metric used is mean absolute distance (MAD)[17], which is used to measure the accuracy of boundary detection. The definition of the MAD is:

$$e(A, B) = \frac{1}{2}[\frac{1}{n}\sum_{i=1}^{n} d(\alpha_i, B) + \frac{1}{m}\sum_{i=1}^{m} d(\beta_i, A)] \tag{10}$$

where $d(\alpha_i, B) = \min_j ||\beta_j - \alpha_i||$. and A, B are two given curves which are presented as sets of points $A = \{\alpha_1, \alpha_2, ..., \alpha_n\}$, and $B = \{\beta_1, \beta_2, ..., \beta_m\}$.

The proposed algorithm obtains 100% accuracy of OD detection on the DRIONS database. Fig.5 shows some detection results chosen from the database randomly where the red lines are the ground truth given by the first specialist, the blue dot and lines are detected by the proposed algorithm. In these cases, the circle detected by the proposed method can fit the OD precisely.

Table 2 gives the quantitative experimental results. The row corresponding to ‘E1’ means the data of the row is taken by using the first observer as the golden standard, and ‘E2’ the second. The ‘Mean’ is the average of ‘E1’ and ‘E2’ in the column direction.

Table 2 The results obtained by the proposed algorithm.

	AOL	TPF	FPF	MAD
E1	0.7933	0.8909	0.135	6.1031
E2	0.7800	0.8911	0.1581	6.4704
Mean	0.7867	0.891	0.1466	6.2868

To illustrate the advantage of the algorithm, we compare the results of the proposed method with those of the method proposed by Walter [10]. To facilitate the

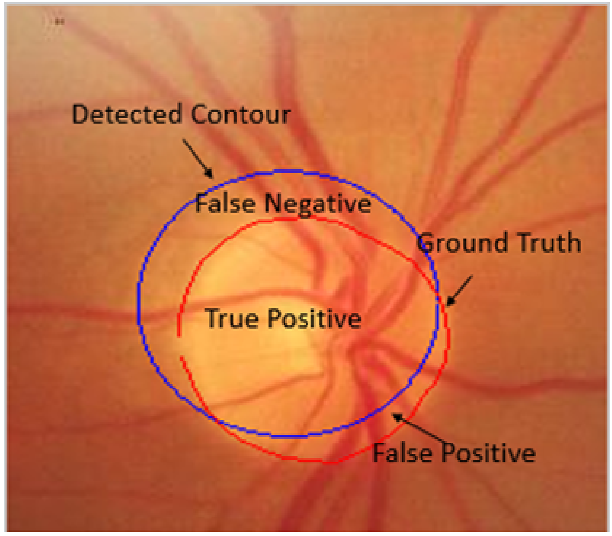

Figure 4 The sketch map to illustrate the basic metrics of TP, FP, and FN.

comparison, the first expert's marks have been taken as the ground truth same as the [3]. Table 3 shows the comparison results. From these results, we can see that in all indicators the proposed method is better than the Walter's method except for FPF. This is mainly because we assume that all the OD size are same, namely, the radius is unchanged when search for the best center. But in fact, this is more reasonable because Walter's method often finds boundary of the OD encompassing a smaller area of the true OD (as illustrated in Figure 6), which leads to a smaller FPF.

Table 3 Comparison of the results achieved by the proposed method and those by the Walter [10].

	Proposed	Walter et al.[10]
AOL	0.7933	0.6227
TPF	0.8909	0.6715
FPF	0.135	0.021
MAD	6.1031	29.6286

DISCUSSION

In this paper, we propose an OD detection method based on the saliency map. Because the region information is used to detect the OD, it is not sensitive to the edge information even when there are very significant false edges in the image that can cause the other algorithm to fail in this circumstance. Fig.6 shows the corresponding instance where Fig.6.(a) is the original image with a notable false edge within the OD. Fig.6.(b) is the result of OD detection using the method proposed by Walter [10]. Fig.6.(c) gives the OD contour (blue line) obtained by the proposed method, in which the red line is the ground truth. By comparing Fig.6.(b) and (c), we can find that the proposed method can detect the OD much better in this circumstance.

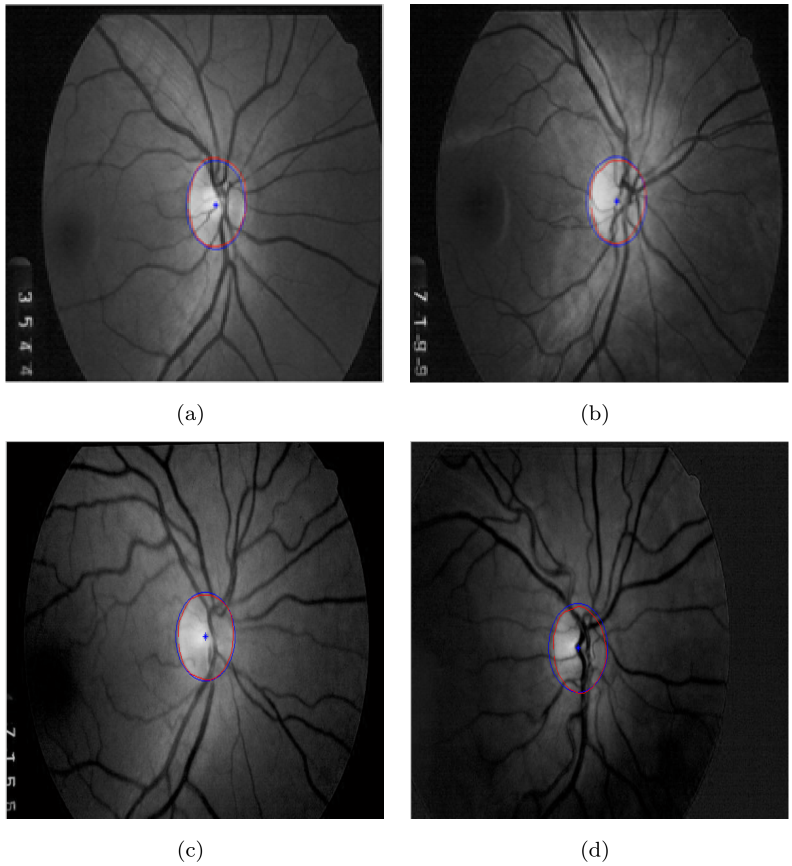

Figure 5 Comparison of the ODs detected by the proposed algorithm and the ODs marked by the specialists. The red lines are the ground truth. the blue dot and lines are detected by the proposed algorithm.

Moreover, based on the fact that the vessels radiate from the OD no matter the illumination is even or not, the proposed method integrates the information of vessels into the region information. Fig.7 shows an example of the corresponding experimental results by using the vessels information and without using the vessels information in the proposed method. It can be seen that the result using the vessels information as illustrated in Fig.7.(b) is much better than the result without using the vessels information Fig.7.(a). This result illustrates that the information of the vessels can play an important role in detecting the OD.

Since the proposed method assumes that the radius of the circle used to fit the OD is known, the main parameters in the proposed method are the threshold values T_1 and T_2. To illustrate the impact of the threshold values on the results, Fig.8 shows the experimental results when T_2 is equal to 0.05 and T_1 is changed from 0.1 to 0.9 with an interval of 0.2. In this interval, the TPF, FPF, and AOL change only slightly, which means that the proposed method is not sensitive to the threshold value T_1. The optimal values (TPF of 0.8674, FPF of 0.1172, AOL of 0.7816) are obtained when T_1 is equal to 0.5.

Fig.9 illustrates a similar case when T_1 is equal to 0.5, and T_2 is changed from 0.01 to 0.2 with an interval of 0.05. Similar with the case in Fig.8, the TPF, FPF

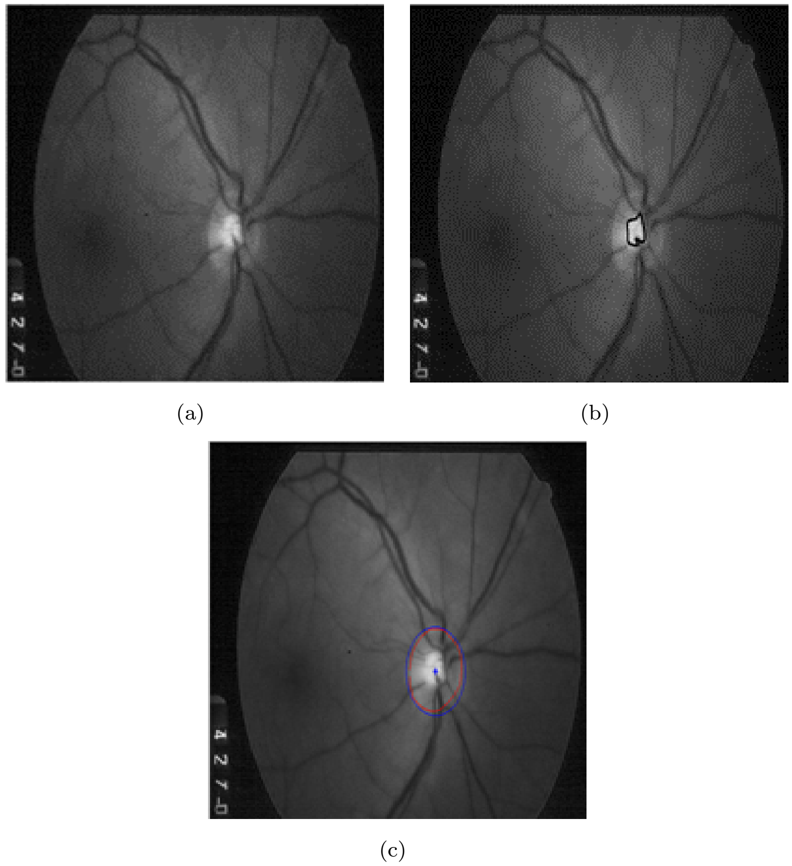

Figure 6 Comparison of the results obtained by the proposed method and the Walter's method: (a) The original image I_g ; (b) The OD detected by Walter[10]; (c) The OD detected by the proposed method.

and AOL change very slightly. When T_2 is equal to 0.1, optimal results are achieved (TPF of 0.8707, FPF of 0.1133, and AOL of 0.7889).

All the above processes are based on the assumption that the radius is known. This might be a disadvantage of the proposed method because not all the OD sizes are the same. Fig.10 gives the results when the radius R is changed from 40 to 50 with an interval of 2 and the T_1, T_2 are fixed to 0.5 and 0.1 respectively. It is notable that when R is less than 46, TPF and AOL increase with increasing R, and FPF changes slowly, which indicates that increasing R is what we want at this stage. But when R is larger than 46, TPF and FPF increase with increasing R, and AOL remains unchanged almost. Even though we obtained a promising value of TPF (TPF=0.9316) when R is equal to 50, the FPF is enlarged also (FPF=0.1823), in general cases it is not so obvious to decide the optimal radius value. How to find a mechanism that can optimize the process of estimating the radius of the OD is one of our future works.

CONCLUSION

In this paper, we proposed a novel method to detect OD based on the saliency map. Experimental results show that the proposed method can detect the center of the

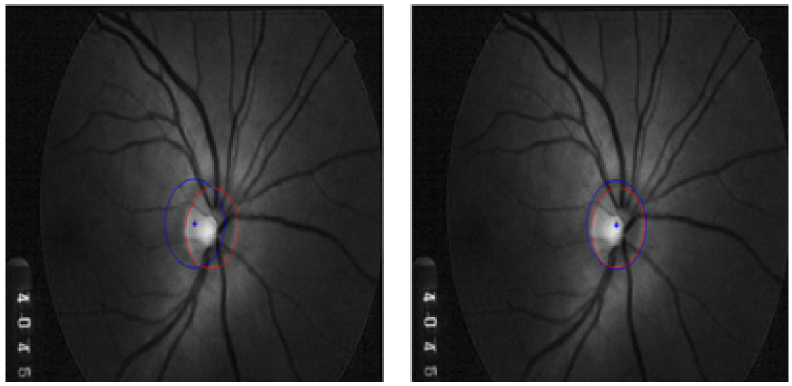

(a) (b)

Figure 7 Comparison of the results using and without using the information of vessels: (a) The result without using the information of vessels; (b) The result using the information of vessels.

OD with an accuracy of 100% in the public dataset DRIONS. In addition, an area overlap of 0.7933, true positive and false positive fraction of 0.8909 and 0.1350, mean absolute distance of 6.1031 are obtained, which outperforms a standard method proposed by Walter [10]. The obtained performance metrics demonstrate that this method is feasible and effective for the automatic segmentation of the optic disk. The sensitivity of the proposed method to the parameters is also studied. It is our plan to automate the process of defining the parameters in our future work.

Competing interests
The authors declare that they have no competing interests.

Author's contributions
Zhun Fan supervised the project, and participated in the design of the algorithm and helped to draft the manuscript. Yibiao Rong and Fang Li carried out the algorithm and collected the data and drafted the manuscript. Xinye Cai, Heping Chen and Weihua Sheng analyzed the results and putted forward modification suggestions.

Acknowledgements
This research work was supported by Guangdong Key Laboratory of Digital Signal and Image Processing, the National Natural Science Foundation of China under Grant (61175073, 61300159, 61332002, 51375287, 61370102, 61170193), Jiangsu Natural Science Foundation (BK20130808).Innovative Application and Integrated Services Platform of the First Generation of Numerical Control in the Eastern Part of Guangdong Province, support no. (2013B011304002).

Author details
[1] Key Laboratory of Digital Signal and Image Processing of Guangdong Province, School of Engineering, Shantou University, Guangdong, China.. [2]School of Computer Science and Technology, Nanjing University of Aeronautics and Astronautics, Jiang Su, China ,. [3]School of Engineering Texas State University, USA.,. [4]School of Electrical and Computer Engineering Oklahoma State University, USA.

References

1. Lu, S.: Accurate and efficient optic disc detection and segmentation by a circular transformation. IEEE Transactions on Medical Imaging **30**(12), 2126–2133 (2011)
2. Lowell, J., Hunter, A., Steel, D., Basu, A., Ryder, R., Fletcher, E., Kennedy, L.: Optic nerve head segmentation. IEEE Transactions on Medical Imaging **23**(2), 256–264 (2004)
3. Morales, S., Naranjo, V., Angulo, U., Alcaniz, M.: Automatic detection of optic disc based on pca and mathematical morphology. IEEE Transactions on Medical Imaging **32**(4), 786–796 (2013)
4. M. Park, J.s.J., Luo, S.: Locating the optic disc in retinal images. IEEE Int. Conf. Comput. Graph. Imag. Visualisat (2006)
5. Aquino, A., Gegundez-Arias, M.E., Marin, D.: Detecting the optic disc boundary in digital fundus images using morphological, edge detection, and feature extraction techniques. Medical Imaging IEEE Transactions on **29**(11), 1860–1869 (2010)
6. Lalonde, M., Beaulieu, M., Gagnon, L.: Fast and robust optic disk detection using pyramidal decomposition and hausdorff based template matching. Medical Imaging IEEE Transaction on **20**(11), 1193–1200 (2001)

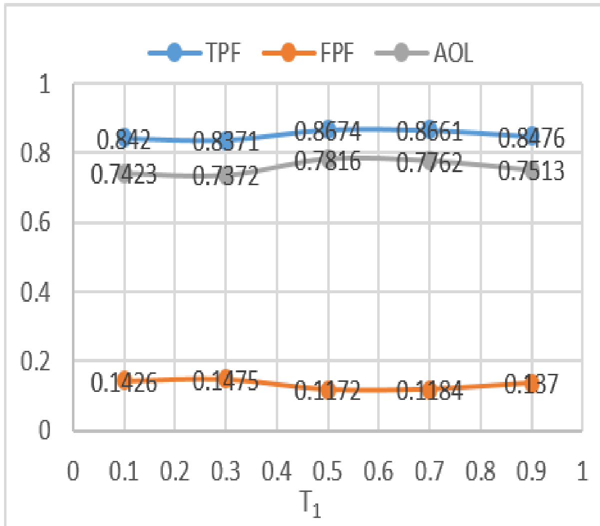

Figure 8 The performance metrics obtained with T_2 is fixed, and T_1 changed from 0.1 to 0.9 with an interval of 0.2.

7. Kauppi, T., Klviainen, H.: Simple and robust optic disc localisation using colour decorrelated templates. In: Proceedings of the 10th International Conference on Advanced Concepts for Intelligent Vision Systems, pp. 719–729 (2008)
8. Osareh, A., Mirmehdi, M., Thomas, B., Markham, R.: Comparison of colour spaces for optic disc localisation in retinal images. In: Pattern Recognition, International Conference On, pp. 10743–10743 (2002)
9. Huiqi, L., Opas, C.: Automated feature extraction in color retinal images by a model based approach. Biomedical Engineering IEEE Transactions on **51**(2), 246–254 (2004)
10. Walter, T., Klein, J.C., Massin, P., Erginay, A.: A contribution of image processing to the diagnosis of diabetic retinopathy detection of exudates in color fundus images of the human retina. IEEE Transactions on Medical Imaging **21**(10), 1236–1243 (2002)
11. Welfer, D., Scharcanski, J., Kitamura, C.M., Pizzol, M.M.D., Ludwig, L.W.B., Marinho, D.R.: Segmentation of the optic disk in color eye fundus images using an adaptive morphological approach. Computers in Biology & Medicine **40**(2), 124–137 (2010)
12. Itti, L., Koch, C., Niebur, E.: A model of saliency-based visual attention for rapid scene analysis. IEEE Transaction on Pattern Analysis & Machine Intelligence **20**(11), 1254–1259 (1998)
13. Harel, J., Koch, C., Perona, P.: Graph based visual saliency. Advances in Neural Information Processing Systems, 545–552 (2006)
14. Malik, . J., Perona, . P.: Preattentive texture discrimination with early vision mechanisms. Journal of the Optical Society of America A **7**(5), 923–932 (1990)
15. Gonzalez, R.C., Woods, R.E.: Digital Image Processing. Addison-Wesley Longman Publishing Co.,Inc.
16. DRIONS-DB: Digital Retinal Images for Optic Nerve Segmentation Database. `[Online].Available:http://www.ia.uned.es/\texttildelowejcarmona/DRIONS-DB.html`
17. Chalana, V., Linker, D.T., Haynor, D.R., Kim, Y.: A multiple active contour model for cardiac boundary detection on echocardiographic sequences. Medical Imaging IEEE Transactions on **15**(3), 290–298 (1996)

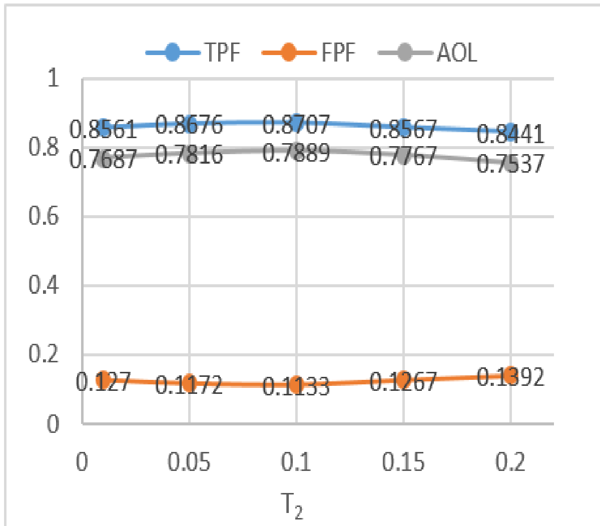

Figure 9 The performance metrics obtained with T_1 fixed, and T_2 changed from 0.1 to 0.9 with an interval of 0.05.

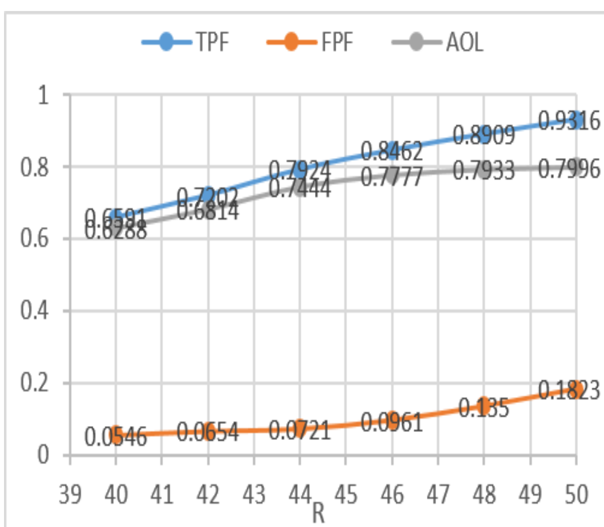

Figure 10 The performance metrics obtained when T_1, T_2 are fixed, and R is changed from 40 to 50 with an interval of 2.